Human Molecular Genetics, 2012, Vol. 21, No. 20 ***4497–4507***
doi:10.1093/hmg/dds292
Advance Access published on July 19, 2012

An X-linked channelopathy with cardiomegaly due to a *CLIC2* mutation enhancing ryanodine receptor channel activity

Kyoko Takano[1,†,‡], Dan Liu[2,†], Patrick Tarpey[3], Esther Gallant[2], Alex Lam[2], Shawn Witham[4], Emil Alexov[4], Alka Chaubey[1], Roger E. Stevenson[1], Charles E. Schwartz[1,*], Philip G. Board[2,¶] and Angela F. Dulhunty[2,¶]

[1]JC Self Research Institute, Greenwood Genetic Center, Greenwood, SC 29646, USA, [2]John Curtin School of Medical Research, Australian National University, Canberra City, ACT 0200, Australia, [3]Wellcome Trust Sanger Institute, Wellcome Trust Genome Campus, Hinxton, Cambridge CB10 1SA, UK and [4]Department of Physics, Computational Biophysics and Bioinformatics, Clemson University, Clemson, SC, USA

Received May 18, 2012; Revised June 29, 2012; Accepted July 12, 2012

Chloride intracellular channel 2 (CLIC2) protein is a member of the glutathione transferase class of proteins. Its' only known function is the regulation of ryanodine receptor (RyR) intracellular Ca^{2+} release channels. These RyR proteins play a major role in the regulation of Ca^{2+} signaling in many cells. Utilizing exome capture and deep sequencing of genes on the X-chromosome, we have identified a mutation in CLIC2 (c.303C>G, p.H101Q) which is associated with X-linked intellectual disability (ID), atrial fibrillation, cardiomegaly, congestive heart failure (CHF), some somatic features and seizures. Functional studies of the H101Q variant indicated that it stimulated rather than inhibited the action of RyR channels, with channels remaining open for longer times and potentially amplifying Ca^{2+} signals dependent on RyR channel activity. The overly active RyRs in cardiac and skeletal muscle cells and neuronal cells would result in abnormal cardiac function and trigger post-synaptic pathways and neurotransmitter release. The presence of both cardiomegaly and CHF in the two affected males and atrial fibrillation in one are consistent with abnormal RyR2 channel function. Since the dysfunction of RyR2 channels in the brain via 'leaky mutations' can result in mild developmental delay and seizures, our data also suggest a vital role for the CLIC2 protein in maintaining normal cognitive function via its interaction with RyRs in the brain. Therefore, our patients appear to suffer from a new channelopathy comprised of ID, seizures and cardiac problems because of enhanced Ca^{2+} release through RyRs in neuronal cells and cardiac muscle cells.

INTRODUCTION

Intellectual disability (ID) results from significant limitations in both intellectual functioning and adaptive behavior and is diagnosed prior to the age of 18. It's prevalence within the general population, worldwide, ranges from 1 to 3% (1). There are many conditions in which ID is a major clinical feature. These conditions are invariably chronic, lasting from the time of onset through the lifetime of the affected individual.

A consistent finding in populations with ID is the excess of males which ranges from 20 to 40% (2–5). If one accepts an excess of males of 30%, one would estimate that X-linked ID (XLID) constitutes one of the most common causes of ID. In fact, XLID is estimated to affect ~2/1000 males (6). XLID is quite heterogeneous, with an estimated 150–200 responsible genes being located on the X-chromosome (7,8). Although steady progress has been made, with more than 90 XLID genes being identified, 30 XLID syndromes and 54 mapped

*To whom correspondence should be addressed. Tel: +1 8649418140; Fax: +1 8643881703; Email: ceschwartz@ggc.org
†K.T. and D.L. contributed equally to the paper.
‡Division of Neurology, Kanagawa Children's Medical Center, Kanagawa, Japan.
¶P.G.B. and A.F.D. made equal senior author contributions to the paper.

families with non-syndromal XLID remain without a gene identification (9). This is likely due to the fact that many of these entities are found in a single family with few affected individuals and mild/moderate cognitive impairment. These features hinder the effectiveness of identifying novel XLID genes employing classical approaches.

Chloride intracellular channel 2 (CLIC2) was first identified as transcript XAP121 located on a transcript map of the region in Xq28 containing the incontinentia pigmenti (*IP2*) gene (10). It was further characterized as being a member of the p64 family with homology to *CLIC1* (11). Members of the CLIC class of chloride channels are related to glutathione transferases, but do not have enzymatic activity. The only physiological function of CLIC2, identified to date, is the inhibition of skeletal ryanodine receptor 1 (RyR1) and cardiac RyR2 channels (12–14). Thus, CLIC2 is thought to play a role in the regulation of Ca^{2+} signaling in cardiac and skeletal muscle as RyRs are the major Ca^{2+} release channels in both muscle types (13) and in other tissues where both the CLIC2 and the RyR proteins are expressed. RyR1 and RyR2 channels are expressed in various areas of the central nervous system, and their dysfunction has been associated with neurological disorders (15,16).

A large collaborative resequencing project of 718 X-chromosome genes in 208 XLID probands was undertaken in an attempt to identify additional XLID genes. This systematic screen identified nine XLID genes based on the presence of multiple truncating variants within a single gene (17). However, the study also identified 531 non-recurrent missense mutations. A partial follow-up of this body of data involved next generation sequencing of 15 probands for the same 718 X-chromosome genes and subsequent analysis of any detected novel missense mutations which were unique (only occurred once). One such missense mutation was identified in *CLIC2*. Follow-up genetic and functional studies indicate that this *CLIC2* mutation is associated with cardiomegaly, congestive heart failure (CHF) as well as seizures and cognitive impairment. These findings point to a critical role for CLIC2 in brain function via its interaction with RyRs.

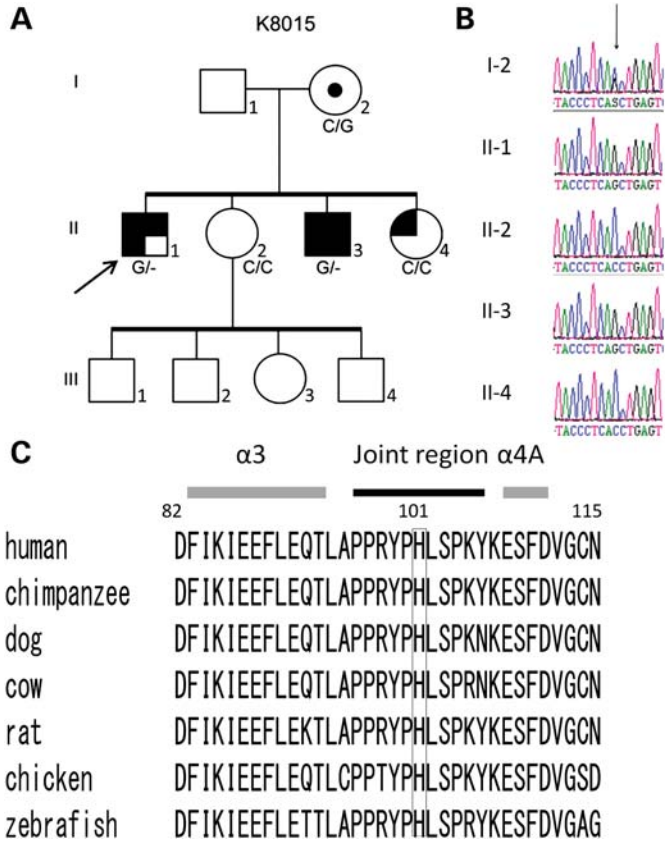

Figure 1. Analysis of *CLIC2* mutation in family K8015. (**A**) Pedigree of K8015. The proband is indicated with an arrow. The genotype (C and/or G) at position c.303 of the *CLIC2* gene is indicated below each individual sequence. Symbols correspond to the following clinical feature: ■, ID; ◪, seizures; ◨, abnormal positioning of the thumb; ◪, macrocephaly. (**B**) Sanger sequencing. Ideograms for individuals in K8015 showing the two affected males and their mother have the position c.303. (**C**) Alignment of CLIC2 protein orthologs. Numbers show the amino acid position of human CLIC2 protein. The H101 position is conserved down to zebrafish. Shaded bars and closed bar indicate α-helices and joint region, respectively.

RESULTS

Mutation in *CLIC2* in family K8015

Next generation resequencing of 718 genes on the X-chromosome identified a c.303C>G (p.H101Q) alteration in a male from a small family with two affected brothers (II-1 and II-3, Fig. 1A). Both had profound ID, large ears and testes and seizures. A sister (II-4) had mild ID (IQ-63) thought to be unrelated to the X-linked condition in her two brothers. Another sister (II-2) was of normal intellectual ability. The mother (II-2) was thought to have a learning disability. As there was some abnormal positioning of the thumbs in both males and one brother had hydrocephalus, *LICAM* sequencing had been conducted which was negative as was Fragile X testing. The *CLIC2* mutation was confirmed by Sanger sequencing in both males and their mother (Fig. 1A and B). The residue is highly conserved down to zebrafish (Fig. 1C). To rule out the possibility that the c.303C>G mutation in *CLIC2* is a rare polymorphism, 1059 X-chromosomes from normal individuals (685 males and 187 females) were screened and none was found to have this alteration.

Cytogenetic analysis

Microarray analysis using the Affymetric Genome-wide Human SNP 6.0 array was conducted on available members of K8015. Affected male II-1 was found to have a copy gain of ~540 kb at 6q27, as did his brother, II-3. This region contains a single gene, thrombospondin II (*THBS2*). Thrombospondins are a family of extracellular glycoproteins that play a role in synaptogenesis (18,19). It is unlikely that a duplication of this gene would give rise to the seizures and cognitive impairment observed in II-1 and II-3. Additionally, II-1 has a loss of 955 kb in 15q11.2. This deletion has been found in patients with developmental and speech delay, mild dysmorphism, behavioral problems including obsessive compulsive behavior, autism and ADHD (20–22). Also, an increased risk for developing generalized epilepsy has been observed in patients with this deletion (23). The brother,

II-3, did not have this CNV. As the affected male II-1 is severely affected, it is unlikely that this deletion is a major contributing factor to his phenotype. II-3 did have a copy loss at 4q13.1 of 226 kb which does not contain any known genes. The sister (II-4) of II-1 and II-3 was found to have only the 4q13.1 loss present in II-3. However, the most compelling evidence against any one of these CNVs being involved in the phenotype, especially the ID, exhibited by the two brothers, is the observation that the normal sister (II-2) was found to have all three CNVs by qPCR.

Tissue expression of CLIC2

CLIC2 is known to be expressed in cardiac and skeletal muscle. However, initial studies found no expression in the human adult brain by northern analysis (24). *CLIC2* expression analysis of human fetal tissue was conducted using RT–PCR and a multiple tissue cDNA panel (Clontech). As shown in Figure 2, *CLIC2* transcript was detected in all fetal tissues, including the brain.

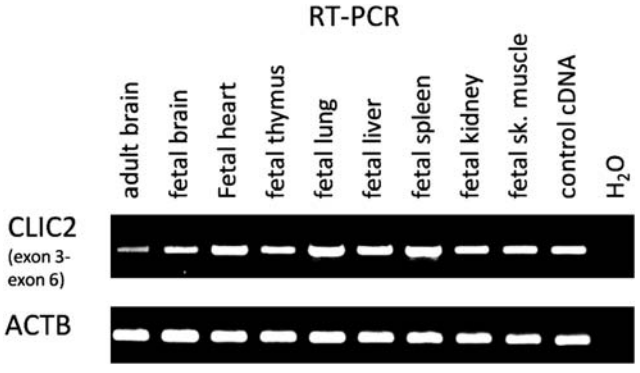

Figure 2. CLIC2 expression. RT–PCR analysis of CLIC2 in various human fetal tissues was conducted using cDNA preparations available in an MTC panel (Clontech) and primers covering exons 3–6. CLIC2 was expressed in all tissues including the fetal brain. It is highly expressed in the fetal lung and spleen. The expression of ACT8 was used as a control.

Immunofluorescent studies of wild-type and mutant CLIC2

The p.H101 residue resides in the joint region between the N-domain and the C-domain of the CLIC2 protein (25). Some *in silico* modeling, using the published crystal structure for the CLIC2 protein, indicated that the p.H101Q alteration would lessen the flexibility of the joint loop reducing its ability to move between soluble and membrane forms, thus affecting the protein's function (26). Immunofluorescent studies were thus conducted in both Cos-7 and PC-12 cells transfected with GFP-tagged mutant *CLIC2*. No differences in protein location, cell morphology or neurite length after the nerve growth factor stimulation of PC-12 cells were observed between wild-type (WT) and CLIC2-H101Q (data not shown). Thus, we undertook additional studies to determine if the CLIC2-H101Q protein functioned differently.

Spectroscopic studies of WT and mutant CLIC2

There was no difference in the endogenous tryptophan fluorescence spectra of the WT and variant proteins (Supplementary Material, Fig. S1A). Similar results were obtained over a pH range from 5.5 to 8. The low pH was tested because of the reported propensity of CLIC2 to form ion channels at low pH. The binding of 1-anilo-8-naphthalene sulfonate (ANS) was used to probe possible changes in conformation that exposed hydrophobic residues. However, the ANS binding spectra obtained for both proteins were identical (Supplementary Material, Fig. S1B). The circular dichroism (CD) spectra of the WT and the variant proteins were also very similar (Supplementary Material, Fig. S1C), indicating that both proteins exhibit the same overall structure. Together, these data suggest that the CLIC2-H101Q variant folds normally.

In contrast to the spectroscopic studies, differential scanning fluorimetry (Fig. 3) revealed a significant increase in the thermal stability of the H101Q variant (CLIC2, $T_m = 46.2 \pm 0.51$; CLIC2H101Q, $T_m = 49 \pm 0.21$; $P = 0.0025$). The increase in thermal stability is possibly indicative of increased structural stability as predicted previously (26).

Effects of WT or H101Q mutant CLIC2 protein on RyR channel activity

As reported previously (12,14,24,27), addition of WT CLIC2 protein to the cytoplasmic (*cis*) side of skeletal RyR1 or cardiac RyR2 channels at concentrations of 4–8 μM, led to a reduction in the activity of both isoforms of the Ca^{2+} release channel (Fig. 4A and B). There was a significant decrease in relative open probability, which can be attributed to an increase in the mean closed time, indicating an increased dwell time in the closed state with little average effect on the duration of the open events (Fig. 4C and D). The H101Q mutation produced a dramatic reversal of the way in which the CLIC2 protein modulated the RyR channels. In marked contrast to the inhibition by the WT protein, the mutant protein increased the activity of both RyR1 and RyR2 channels (Fig. 4A and B), with a significant increase in the open probability in both isoforms of the channel (Fig. 4C). In skeletal RyR1 channels, this was due to a significant increase in the mean open time of the channel and a significant decrease in the mean closed time (Fig. 4D and E) which would result in an increase in the frequency of the longer events. The changes in open and closed times in the cardiac RyR channels in the presence of the H101Q mutant CLIC2 protein were more variable than those in the skeletal channels, and although there was a trend toward an increase in mean open time, this was not statistically significant.

RyR–CLIC2 binding energy changes due to H101Q mutation

The three-dimensional structure of the RyR–CLIC2 complex was predicted with ZDOCK. ZDOCK generates a set of structures ranked according to the ZDOCK scoring function. To assess the effect of small structural variations, the calculations of the binding free energy were done by using both the top-ranked ZDOCK prediction and the 10 best predictions

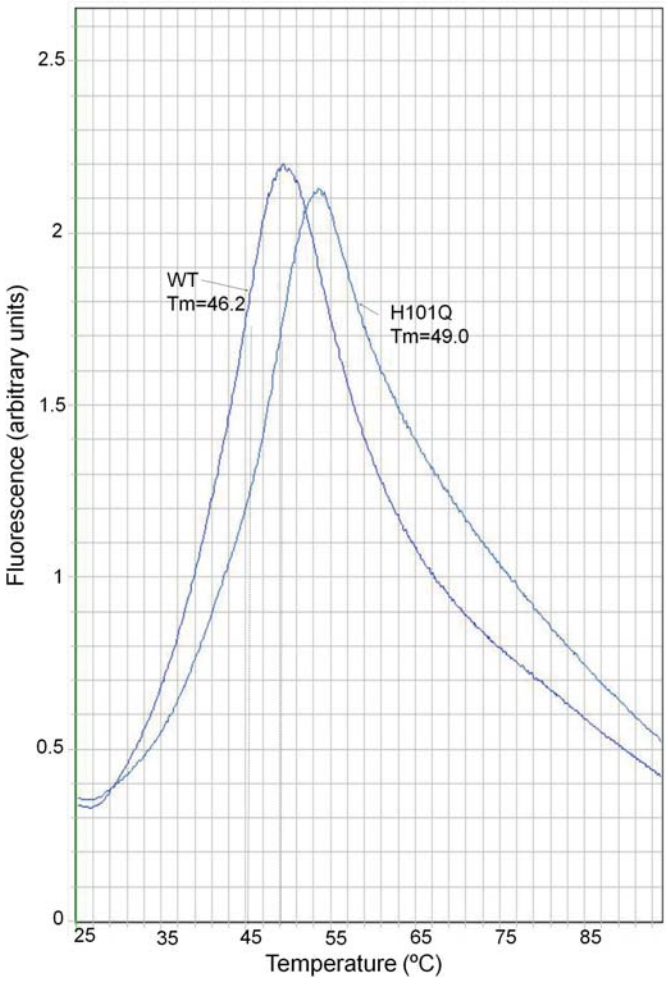

Figure 3. Heat denaturation of CLIC2 and the H101Q. Heat denaturation of CLIC2 and the H101Q variant determined by differential scanning fluorimetry with SYPRO orange. The vertical dashed lines indicate the T_m. The spectra are representative of triplicate determinations.

(Table 1). It was found that RyR–CLIC2 binding affinity is affected by the H101Q mutation, since residue 101 is quite close to the interface of the RYR domain 5 (D5)–CLIC2 complex as inferred from both the ZDOCK 3D structure prediction and previous cryo-electron microscopy (14). The energy calculations, excluding the entropy term, suggest that the CLIC2-H101Q variant binds more strongly to the D5 region of RyR when compared with the WT CLIC2 protein (Table 1; a positive $\Delta\Delta G$ means more stable binding). Additionally, folding free energy calculations have predicted that H101Q mutant is more stable (26). Cryo-electron microscopy experiments have suggested that CLIC2 may induce conformation changes in RyR (14) and electrophysiological experiments showed that RyR, in the presence of CLIC2-H101Q, has a higher open probability (and would release more Ca^{2+}) than RyR in the presence of WT CLIC2. Therefore, CLIC2-H101Q must still bind to RyR in a manner that favors the open state of the RyR channel. This may be achieved by an increased binding affinity (compared with WT CLIC2) as well as an increase in its stability.

Ion channels formed by the CLIC2 protein

When purified WT or H101Q mutant, CLIC2 protein was added to the bilayer solution at concentrations of between 0.24 and 1.2 μM, channel activity was observed after periods ranging from several seconds to many minutes. The bilayer solution was set at pH 5 and contained 1–5 mM oxidized glutathione (GSSG), since channel incorporation had previously been shown to be facilitated by acid pH and oxidizing conditions (28).

Channel openings to a range of current levels were observed (Fig. 5A–D), with unitary events having a conductance of 16.2 ± 0.7 pS for the WT protein and 14.3 ± 0.7 pS for the H101Q mutant CLIC2 protein, averaged over the full voltage range from +120 to −120 mV. The difference between the unitary conductances for WT and mutant channels was small but significant. The unitary conductance of both WT and mutant channels was smaller than the single channel conductance of ∼48 pS reported by Cromer *et al*. (28) using the tip–dip method of channel recording. It is not clear in our study if the unitary conductance was in fact a single channel conductance or a subconductance level as no recordings were obtained of unitary events only with either the WT or the mutant CLIC2. The channels formed by both proteins exhibited a range of gating modes characterized by either synchronized openings to levels that varied between 1 and >20 times the unitary current (Fig. 5A–D) or asynchronous openings to the same levels which often occurred within a few seconds of the synchronous openings (Fig. 5A). Examples are shown of different types of gating between lower conductance levels at different times in Figure 5B and C during the same WT CLIC2 experiment as that shown in Figure 5A.

One interpretation of the gating behavior seen in these experiments is that rafts of channels incorporated into the bilayer and that their opening was at times coordinated (when synchronous openings were observed) and at other times not coordinated. Such behavior might be explained if coordinated openings were seen when all proteins in the raft adopted an appropriate orientation to each other, and asynchronous openings when this orientation was disrupted. Indeed, such rafts have been described in synaptic proteins (29–31).

The current–voltage relationship for the unitary currents from both WT and H101Q mutant CLIC2 channels demonstrated a simple linear relationship (Fig. 5E). The current voltage relationship for maximum current was also linear for the WT CLIC2 channels (Fig. 5F). On the other hand, the maximum conductance of the H101Q mutant channels was very variable and the maximum current amplitude decreased significantly between 70 and 90 mV at both positive and negative potentials. As this reduction at more extreme potentials was not seen in the unitary current, the result suggests that multiple channel opening was suppressed at larger voltages in the H101Q mutant channels.

Although the conductance and overall gating behavior of the WT and H101Q mutant CLIC2 proteins was similar, a consistent difference was noted in the ease with which the channels incorporated into the bilayer and the length of time that channels were recorded before bilayer breakage. Bilayer breakage often appeared to be associated with a sudden increase in the current when a massive number of

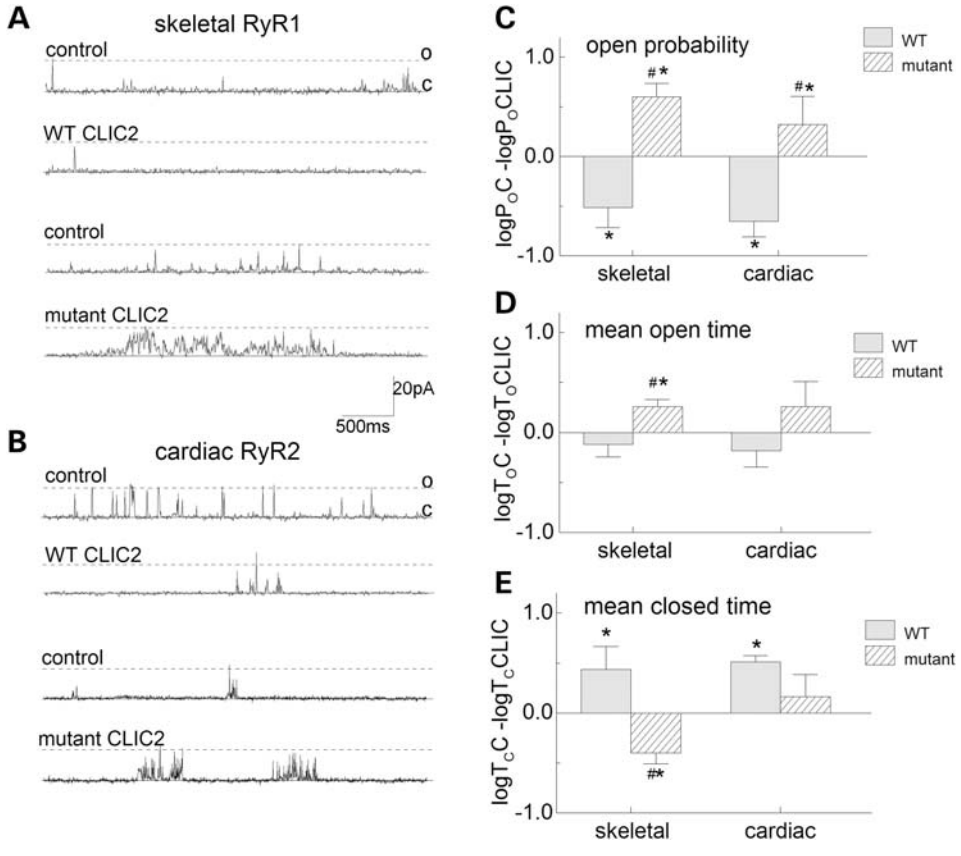

Figure 4. Actions of WT and H101Q mutant CLIC2 channels on skeletal RyR1 and cardiac RyR2 channels incorporated into lipid bilayers. (**A**) Three second current recordings from skeletal RyR1 channels at pH 7.2. Activity of one channel before and after exposure to WT CLIC2 (upper two records) and a second channel before and after exposure to the H101Q mutant protein (lower records). (**B**) Records of 3 s of activity from cardiac RyR2 channels. Activity of one channel before and after exposure to WT CLIC2 (upper two records) and from a second channel before and after exposure to the H101Q mutant protein (lower two records). In (A) and (B), channel activity is recorded at +40 mV and channel opening is upward from the closed level (c) to the maximum single channel current (broken line, o). Effects of average relative open probability (**C**), mean open time (**D**) and mean closed time (**E**). For each parameter the logarithm (to the base 10) of the relative change is shown. For example, the log of the control open probability (log P_oC) is subtracted from the log of the open probability in the presence of CLIC2 (log P_oCLIC) was calculated for each channel and average data presented. The log relative P_o is given to reduce the effect of the normal variability in control RyR channel activity (58). The asterisk indicates a significant difference from control and the hash symbol indicates a significant difference between the effects of the WT CLIC2 and the H101Q mutant protein.

Table 1. $\Delta\Delta G$ calculation of the top prediction given by ZDOCK and the average of all top 10 predicted complexes

	Complex (2XOA_2PER)	Receptor (2XOA)	Ligand (2PER)	ΔG (kcal/mol)	$\Delta\Delta G$ (kcal/mol)
Top prediction					
WT	−22 490.0896	−15 162.2826	−7341.6016	13.7946	9.5492
H101Q	−22 512.4834	−15 162.2826	−7354.4462	4.2454	
Top 10 Average					
WT	−22 506.6473	−15 162.2826	−7341.6016	−2.7631	4.8641
H101Q	−22 524.35601	−15 162.2826	−7341.6016	−7.62721	

additional channels opened. These observations are quantified in Table 2. The data show that the WT protein incorporated twice as often as the mutant protein, although the mean time required for incorporation was much the same. Once incorporated, the WT channels were recorded for twice as long as the H101Q mutant channels, largely due to bilayer breakdown with additional incorporation or opening of the mutant channels.

DISCUSSION

Channelopathies are a large collection of human disorders that are caused by mutations in various genes encoding ion channels or their regulatory proteins (32). These disorders cover a wide range of symptoms and etiologies. One group of channelopathies results from defects in calcium channels. Within this constellation of calcium channelopathies, there are those

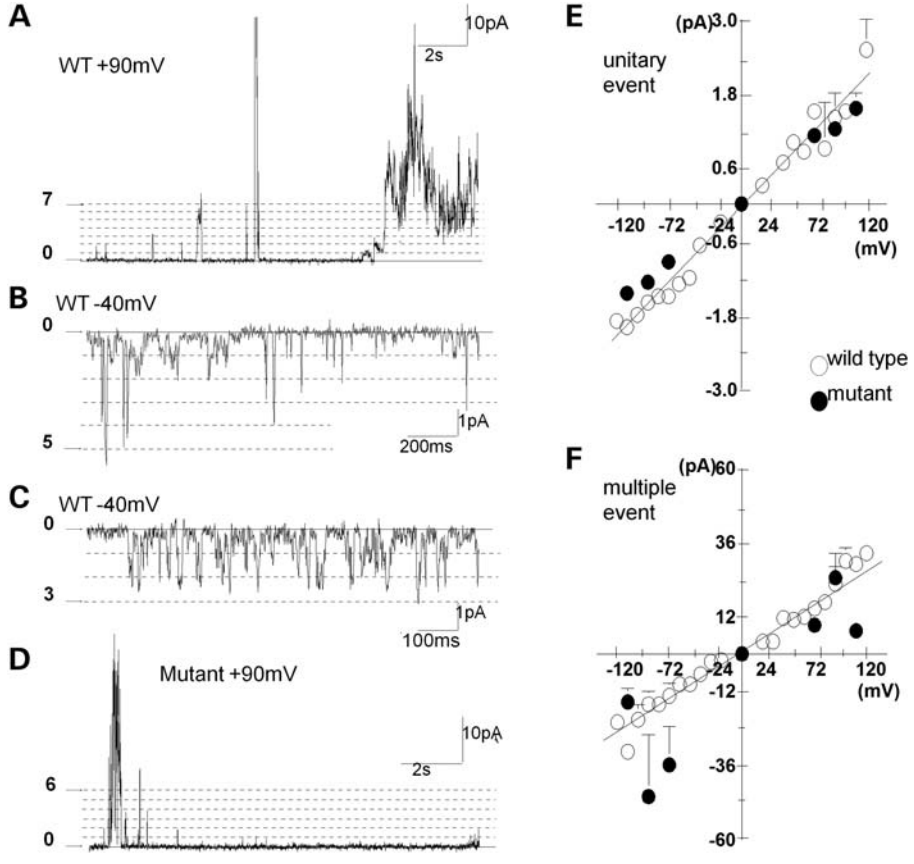

Figure 5. WT and H101Q mutant CLIC2 channel activity recorded at pH 5.0 with 1 mM GSSG. (**A**–**D**) Current recordings following the incorporation of CLIC2 channels. The broken lines indicate conductance levels which were multiples of the unitary conductance [~2 pA at +90 mV in (A) and (D) or ~1 pA at −40 mV in (B) and (C)]. (A–C) Examples of different gating modes recorded during one experiment in which WT CLIC2 protein was added to the bilayer solution. (A) Continuous 16 s recording in which the channel is initially opening to the unitary conductance or multiples up to 7× the unitary conductance. After ~8 min, there is a coordinated opening to ~30× the unitary conductance. Finally, after ~13 min, a prolonged burst of uncoordinated activity reaching the same maximum levels. (B) Approximately 5 min later in the experiment, periods of opening to levels 1–5 were apparent. (C) After a further 5 min, there were more rapid openings between levels 0 and 3. (D) A recording from a bilayer following incorporation of H101Q mutant CLIC2 channels. The gating is similar to that seen in the WT channel shown in (A). Average current–voltage relationship of unitary events (**E**) and maximal currents (**F**) for WT CLIC2 channels (open circles) and H101Q mutant CLIC2 channels (filled circles).

Table 2. Comparison of incorporation parameters for WT and H101Q mutant CLIC2 channels

	Number of attempts	Number of incorporations	Total observation time (min)	Mean time before incorporation (min)	Mean bilayer lifetime after incorporation (min)
WT CLIC2	56	23	987	4.8 ± 0.9	12.1 ± 3.9
Mutant CLIC2	46	12	1114	6.4 ± 2.3	5.8 ± 1.7

There were fewer incorporations with the mutant channels and the bilayer broke sooner (often due to massive channel incorporation) than with the WT protein.

with mutations in voltage-gated calcium channels (33) and in the ligand-gated RyRs (34–36). The CLIC2 H101Q mutation results in a channelopathy which becomes a member of this second group.

The lack of an effect on tryptophan fluorescence, ANS binding or the CD spectrum indicates that the H101Q mutation does not result in any overall structural change in the protein, but that the variant protein may have a greater than normal structural stability. This increased structural stability was predicted by previous *in silico* analysis (26). The increased structural stability may lead to stronger binding of H101Q CLIC2 mutant to the RyR. Although this was not specifically examined, it is clear that there is no major decrease in affinity as the same concentration of WT and mutant protein both caused significant functional changes in RyR activity. A similar or tighter binding of the mutant protein would prevent other CLIC isoforms from binding to the RyRs to possibly compensate for the mutation in CLIC2, if indeed other isoforms act in the same manner as CLIC2. As yet, there are no reports of other CLIC isoforms regulating RyR activity.

The CLIC2 protein acts as a negative regulator of RyR channels and presumably Ca^{2+} release through the channels. However, our data indicate that the mutant CLIC2-H101Q protein would stimulate the release of Ca^{2+} by keeping the RyR channel in an open state, possibly due to a higher binding affinity for the RyR protein. The reversal of the normal function of CLIC2 on RyR channels by the H101Q variant protein would have a drastic effect on Ca^{2+} signaling in any cells whose function is dependent on Ca^{2+} released from internal stores through any of the RyR receptor isoforms (RyR1, RyR2 and probably RyR3). Overly active RyRs in the heart leads to excess action potential firing in those cells. Consistent with this fact, both affected males suffered from cardiomegaly and congestive heart disease. Patient II-1 also experienced atrial fibrillation which contributed to his death.

Leaky RyR2 channels associated with some gene mutations can result in seizures because of RyR2's location in Purkinje cells and the cerebral cortex (37–39). Thus, an overall affect of overly active RyRs in these same cells, as well as the hippocampal neurons (38–40), might trigger excessive neurotransmitter release and affect other post-synaptic pathways involved in plasticity, memory and learning. In mouse, knocking out RyR3 resulted in deficits in special learning (41,42). Hippocampal tissue also exhibited lower initial amplitude of potentiation and impaired long T potentiation maintenance, suggesting that RyR3 has a functional role in synaptic plasticity (42). Thus, impaired RyR activity in certain neurons due to the CLIC2 H101Q variant could account for our patients' seizures and cognitive impairment. The mother of the two affected males is a carrier of the CLIC2 H101Q variant and was reported to have a learning disability. This may have been a result of the CLIC2 alteration as she had random X-inactivation. Unfortunately, she is no longer alive and her medical records are not available to determine if she experienced any cardiac problems. Her mildly impaired daughter (II-4) does not carry the CLIC2 H101Q variant, had highly skewed X-inactivation and does not have any X-chromosomal abnormalities associated with ID. The highly skewed X-inactivation in person II-4 suggests that she has an X-linked mutation of significance. However, as the X-exome sequencing of her bothers failed to identify any potentially pathogenic changes other than the CLIC2 H101Q mutation, it is unlikely that an X-linked mutation carried by her is contributing to the ID phenotype in her severely affected brothers. With respect to other possible explanations for the ID in this family, as whole exome sequencing of all family members was not undertaken, there remains the possibility that the ID exhibited in the two affected males is not X-linked.

Although skeletal muscle abnormalities were not documented, they may have not been particularly apparent given the more compromising cardiac and cognitive phenotype. Although the stimulatory effect of the CLIC2 mutation RyR channel activity is the most likely mechanism underlying the cardiac and cognitive defects, effects on other mechanisms in patient's tissues cannot be ruled out.

In silico analysis of the WT and H101Q mutant protein predicted an increased stability of the mutant protein that might hinder its insertion into the membrane to form an ion channel (26). Our data show that this is indeed the case and further suggest that once the mutant protein is inserted into the membrane, it can facilitate the insertion of additional protein. The effect of this on function is speculative since, as far as we know, the function of CLIC2 channels (seen mostly under low pH conditions and with excess oxidation) is not known. However, our data show that there are changes in channel activity and ability to insert into bilayers and that this could affect function. This is the first report of CLIC2 channel aggregation in membranes. Such aggregation of ion channels is not uncommon and has been reported in synaptic ion channels (29), in extrasynaptic GABA receptors channels (30) and in purified and native RyR channels (31). The role of such aggregation is thought to allow for focused ion current flow to microdomains within the cell and for greater potential for the functional regulation of the currents. Again the role of aggregation in CLIC2 channel function remains to be determined.

In summary, the H101Q variant of CLIC2 adversely affects its regular inhibitory action of RyR activity and hence affecting Ca^{2+} release through RyRs and Ca^{2+} signaling in cells critical to cognitive function. Since it has been proposed that human diseases resulting from mutations in proteins that regulate ion channels can be defined as channelopathies (32), this X-linked condition can be considered a novel channelopathy that is also associated with cardiomegaly and congestive heart disease.

MATERIALS AND METHODS

Clinical evaluation of K8015

The mother (I-2, Fig. 1A) attended school until the seventh grade and was considered by family members to have a learning disability.

The oldest brother, II-1, was globally delayed in development. He showed poor head control as an infant, walked at 2 years and had only a few words at 4 years. Seizures began in infancy. He experienced a 'flu-like' illness at 8 months with high fever. He was admitted to a residential institution at age 4.6.

During adult life, his speech was limited to single words, phrases and a few sentences. Hearing was considered adequate for speech perception. From his early 40s, his heart was at the upper limits of normal size. In his early 70s, he had CHF with atrial flutter requiring cardioconversion. The right heart was dilated and there was mild mitral and tricuspial insufficiency and mild aortic stenosis. Cataracts were present at 72. A brain MRI was normal. He had large joint contractures and kyphoscoliosis. He had profound ID with an IQ measured as 6. He died at age 73 of CHF, atrial fibrillation and pneumonia.

The younger brother, II-3, was also globally delayed, walking at 2 years and beginning to talk at 3 years. He was institutionalized at age 4. At age 43, he had mitral valve prolapse and mild left ventricular hypertrophy. The heart size was mildly enlarged from his mid-40s and he had periodic CHF from his mid-50s. He also has seizures, was mute and had spastic quadriplegia with large joint contractures. He has profound ID with an IQ of 2.

Exon capture and deep sequencing

Genomic DNA (5 μg) was fragmented by Adaptive Focused Acoustics on a Covaris E120 (Covaris Inc., Woburn, MA, USA) for 90 s with a duty cycle of 20%, intensity of 5 and cycles per burst of 200. The fragmented DNA was purified using a Qiaquick PCR purification column (Qiagen, Valencia, CA, USA, 28 104) and quantified on a Bioanalyser using the Agilent DNA 1000 kit (Agilent, 5067-1504). The resulting DNA ranged in size from ∼100 to 400 bp, with a modal fragment size of ∼250 bp. Genomic libraries were prepared using the Illumina Paired End Sample Prep Kit following the manufacturer's instructions (Illumina, San Diego CA, USA). Adapter-ligated DNA was purified using AMPure beads (Agencourt BioSciences Corporation, Beverly, MA, USA) following the manufacturer's protocol and eluted in 40 μl of nuclease-free water. The prepared library was used directly in the subsequent enrichment procedure without prior size selection or PCR amplification.

The genomic library (500 ng) was mixed with 7.5 μg of human C_0t1 DNA, lyophilized in a speedvac for 30 min at 45°C and rehydrated in 3.4 μl of nuclease-free water. Enrichment of the genomic DNA was performed using the Agilent SureSelect Human X Chromosome kit corresponding to the exons annotated within the consensus CDS database with minor modifications to the manufacturer's protocol. Briefly, the genomic DNA library (3.4 μl) was combined with 2.5 μl of block reagent 1, 2.5 μl of block reagent 2 and 0.6 μl of block reagent 3 and transferred to a well of a microtitre plate. The sample was denatured by incubating the plate on a thermocycler at 95°C for 5 min then snap-cooled on ice. A hybridization mix was prepared comprising 25 μl of Hyb reagent 1, 1 μl of Hyb reagent 2, 10 μl of Hyb reagent 3 and 13 μl of Hyb reagent 4. A 13 μl aliquot of this mastermix was added to the denatured DNA, and the sample incubated at 95°C for 5 min, then 65°C for 5 min. In a separate microtitre plate, the baits were prepared by combining 5 μl of SureSelect capture library with 1 μl of nuclease-free water and 1 μl of RNAse block, and the plate incubated at 65°C for 3 min. The pre-warmed DNA (22 μl) was transferred to the pre-warmed bait mix and the solution incubated for 24 h at 65°C. Following hybridization, the captured DNA was isolated using streptavidin-coated magnetic Dynabeads (Invitrogen, 653.05) and washed following the standard Agilent SureSelect protocol. The isolated DNA was purified using a Qiagen MinElute purification column, eluted in 15 μl of elution buffer and PCR amplified for 14 cycles as described previously (43).

Oligo-microarray analysis

Genomic DNA was isolated from peripheral blood using Qiagen DNA minikit (Qiagen). The quality and quantity of the isolated DNA was assessed by agarose gel electrophoresis and spectrophotometric analysis, respectively. DNA microarray was performed employing the Affymetrix Genome-wide SNP 6.0 platform according to the manufacturer's instructions (Affymetrix Inc., Santa Clara, CA, USA). Briefly, 250 ng genomic DNA is digested with the restriction enzymes *Sty*I and *Nsp*I, each, and ligated to a common adaptor with T4 DNA ligase. Following ligation, the template is subjected to PCR using TITANIUM™ Taq-DNA polymerase. The PCR products of both enzymatic reactions are pooled and purified, and then fragmented with Fragmentation Reagent (DNAse I), and end-labeled using terminal deoxynucleotidyl transferase. Subsequent to hybridization, the array was washed and stained in the GeneChip® Fluidics Station 450 and scanned with a GeneChip® Scanner 3000 7G using the Affymetrix Genome-wide SNP 6.0 array protocol. Copy number analysis was performed with Affymetrix's Genotyping Console 4.0 (GTC 4.0) using the *in silico* control of 270 HapMap samples.

Confirmation of CLIC2 variant

The c.303C>G variant in *CLIC2* was confirmed using Sanger Sequencing in a second sample of genomic DNA. Once confirmed, other members of family 8015 were also sequenced.

Polymorphism analysis

Screening of normal control individuals (males and females) for the c.303C>G variant consisted of digesting amplified genomic DNA with *Hha*I. The c.303C>G alteration creates a *Hha*I site such that a 263 bp PCR fragment is digested into two fragments of 201 and 62 bp. Digested DNA was visualized using a 1% agarose gel.

CLIC2 tissue expression analysis

Human Fetal MTC panel (Clontech) was utilized for the analysis of CLIC2 expression in fetal tissues. The MTC cDNA preparations utilized for RT–PCR analysis were conducted as outlined by the manufacture in a final reaction volume of 20 μl. Primers for *CLIC2* were RT-F 5′-AGGTACCAATCCTCCGTTCC-3′ and RT-R 5′-TCAGGACACGTGTGGGTAAA-3′. Primers for the control gene, *ACTB* were RT-F 5′-ATGGGTCAGAAGG ATTCCTATGTG-3′ and RT-R 5′-TGTTGAAGGTCTCAAA-CATGATCTGG-3′. PCR conditions for *CLIC2* were: initial denature 95°C for 5 min, followed by 30 cycles of denature at 95°C for 30 s, annealing at 57°C for 30 s and extension at 72°C for 40 s. Final extension was at 72°C for 5 min. For *ACTB*, the PCR conditions were the same except the annealing was done at 55°C, the extension was for 30s and only 25 cycles were used. About 10 μl of the PCR was run on a 3% agarose gel in 1× TBE.

Expression and mutagenesis of recombinant CLIC2

Recombinant CLIC2 was expressed in *Escherichia coli* from a pHUE vector and purified by Ni-agarose affinity chromatography as described previously (44). This strategy provides recombinant CLIC2 without any additional residues. The purified CLIC2 protein and its H101Q variant were adjusted to 6 mg/ml in N-(Hydroxyethyl)piperazine-N′s-(2-ethanesulfonic acid) (HEPES) buffer (50 mM HEPES, pH 7.4, 200 mM KCl and 10% glycerol).

Mutagenesis was undertaken by the overlapping PCR method using the following primers: MutF, 5′-TCCAA GGTACCCTCAGCTGAGTCCCAAGTACA-3′; MutR, 5′-TGT ACTTGGGACTCAGCTGAGGGTACCTTGGA-3′; CLIC2F, 5′-CGCGGATCCGGCCTGCGGCCCGGCACT-3′; and CLIC2R, 5′-TTGCATAAGCTTAAGCCACATTTGCGTA-3′.

The presence of the desired mutations and the absence of additional mutations were confirmed by DNA sequencing.

Circular dichroism

The WT CLIC2 and mutated form (H101Q) were diluted to 0.5 mg/ml in 10 mM phosphate buffer and pH adjusted to 8.0. CD spectra were collected at 20°C on a Chirascan CD spectrometer (Applied Photophysics Ltd, Leatherhead, Surrey, UK). Three spectra were collected, averaged and subjected to a smoothing function.

Fluorescence scanning

Fluorescence spectra were determined in a LS50B Luminescence Spectrophotometer (Perkin Elmer, USA) with a protein concentration of 5 μM. For endogenous tryptophan fluorescence, the excitation wavelength was set at 280 nm and the fluorescence spectrum was obtained from 290 to 450 nm. The hydrophobic fluorescence probe 1-aniliano-8-naphthalene sulfonate (ANS; Fluka analytical, Castle hill, NSW, Australia) was used at a final concentration of 50 μM to assess whether the conformational changes occurred as a result of the H101Q mutation. The protein solutions (5 μM) were incubated with the dye for 50 min at room temperature and were then scanned. The excitation wavelength was set at 390 nm, and the fluorescence spectrum was obtained from 405 to 540 nm.

Differential scanning fluorimetry

The thermal stabilities of CLIC2 and its H101Q variant were determined by measuring the fluorescence of SYPRO orange during thermal denaturation from 25 to 95°C with ramp rate 1°C/min (36,45). Briefly, proteins were diluted to 0.1 mg/ml in HEPES buffer. Diluted SYPRO orange (1:1000) was added to the protein solution (20 μl), and the mixtures were heated while monitoring the fluorescence on a 7900HT fast real-time PCR system (Applied Biosystems). Fluorescence excitation was at 470 nm and detection was at 555 nm. The raw data were analyzed with 7900HT software and the first derivative calculated to determine T_m.

RyR isolation and single channel experiments

Cardiac sarcoplasmic reticulum (SR) was prepared from the sheep heart (46). Skeletal SR was isolated from the back and leg muscles of New Zealand White rabbits, and heavy SR was collected from the 35–45% (wt/vol) interface of a discontinuous sucrose gradient, centrifuged and resuspended (24,47–50). Ion channel activity was recorded following microsomal vesicle incorporation into artificial lipid bilayers separating *cis* and *trans* solutions containing symmetrical 250/250 mM Cs^+ with $CH_3O_3S^-$ as the major anion (24). *Cis* Ca^{2+} was 10 μM with ~2 mM 1,2-bis(O-aminophenoxy)ethane-N,N,N′,N′-tetraacetic acid (BAPTA). The Ca^{2+} concentration was confirmed using a Ca^{2+} electrode. *Trans* Ca^{2+} was 1 mM. Bilayer potential is expressed as the voltage in the cytoplasmic solution relative to luminal solution and was changed every 30 s between +40 and −40 mV. Single channel parameters were obtained using the channel 2 program (developed by P.W. Gage and M. Smith, John Curtin School of Medical Research, Canberra, Australia) (51). Current was recorded at 5 kHz and was filtered at 1 kHz. Channels were blocked by ruthenium red at the end of the experiment to confirm that they were RyRs.

Binding of RyRE-CLIC2 modeling

Using the PDB 2XOA (Supplementary Material, Fig. S2) as the model for the N-terminal region of RyR (which consists of D5) (52), docking predictions were done between CLIC2 and 2XOA. Using the ZDOCK software (53,54), the top 10 predictions were determined. The diagram in Supplementary Material, Figure S3, shows the N terminus of CLIC2 as its binding interface, along with the first 206 amino acids as the RyR 2XOA binding interface. This binding region of RyR is a beta barrel-like region, which corresponds to D5 in Serysheva *et al*. (52). The entire 2XOA structure was used for the binding predictions.

The energy of the RyR–CLIC2 complex was determined by using the minimize.x module within the TINKER Molecular Dynamics Package. The change in the difference of folding free energy ($\Delta\Delta G$) was determined by:

$$\Delta\Delta G = (\Delta G\_\text{complex\_WT}) - (\Delta G\_\text{complex\_H101Q}) \quad (1)$$

where ΔG_complex_WT and ΔG_complex_H101Q are defined to be the difference in folding free energy of the complexes consisting of CLIC2-WT and CLIC2-H101Q ligands, respectively. More precisely, ΔG_complex_WT/H101Q is given by (for more details see 55–57):

$$\Delta\text{G\_complex\_WT/H101Q} = \text{G\_RyR} - \text{CLIC2\_complex} - \text{G\_RyR} - \text{G\_CLIC2\_WT/H101Q} \quad (2)$$

CLIC channel recording

Lipid bilayers were formed as described above. The *cis* and *trans* solutions had the same composition and contained (140 mM KCl, 1.5 mM $MgCl_2$, 10 mM HEPES, pH 5.0). In most experiments, GSSG was added to the *cis* chamber and this increased pH to 5.5. WT or H101Q mutant CLIC2 protein was added to the *cis* chamber and the solution stirred until channel activity was observed.

Statistics

Average data are presented as the mean ± SEM. The significance of differences between control and test values were tested using a Student's *t*-test for paired data or unpaired data, as appropriate. A *P*-value of <0.05 was considered significant.

SUPPLEMENTARY MATERIAL

Supplementary Material is available at *HMG* online.

ACKNOWLEDGEMENTS

We thank the family for their participation in our study of X-linked intellectual disability. Joan Montjoy and Cindy

Skinner assisted with follow-up studies of the family. Dedicated to the memory of Ethan Francis Schwartz, 1996–1998.

Conflicts of Interest statement. None declared.

FUNDING

This work was supported in part by a grant from the National Institutes of Health (National Institute of Child Health and Development) (HD26202 to C.E.S.); a grant from the South Carolina Department of Disabilities and Special Needs (SCDDSN); a grant from the Australian National Health and Medical Research Council (1008477 to P.G.B. and A.F.D.) and a grant from the National Institutes of Health (National Institute of General Medical Sciences) (GM09392 to E.A.).

REFERENCES

1. Leonard, H. and Wen, X. (2002) The epidemiology of mental retardation: challenges and opportunities in the new millennium. *Ment. Retard. Dev. Disabil. Res. Rev.*, **8**, 117–134.
2. Penrose, L. (1938) A clinical and genetic study of 1280 cases of mental defect. Special Report Series. Medical Research Council No. 229. Her Majesty's Stationery Office, London.
3. Lehrke, R. (1974) X-linked mental retardation and verbal disability. *Birth Defects Orig. Artic. Ser.*, **10**, 1–100.
4. DS Herbst, J.M. (1980) Nonspecific X-linked mental retardation II: the frequency in British Columbia. *Am. J. Med. Genet.*, **7**, 461–469.
5. Stevenson, R.E. (2000) Splitting and lumping in the nosology of XLMR. *Am. J. Med. Genet.*, **97**, 174–182.
6. Ropers, H.H. and Hamel, B.C. (2005) X-linked mental retardation. *Nat. Rev. Genet.*, **6**, 46–57.
7. Stevenson, R.E., Abidi, F., Schwartz, C.E., Lubs, H.A. and Holmes, L.B. (2000) Holmes-Gang syndrome is allelic with XLMR-hypotonic face syndrome. *Am. J. Med. Genet.*, **94**, 383–385.
8. Chiurazzi, P., Schwartz, C.E., Gecz, J. and Neri, G. (2008) XLMR genes: update 2007. *Eur. J. Hum. Genet.*, **16**, 422–434.
9. Lubs, H.A., Stevenson, R.E. and Schwartz, C.E. (2012) Fragile X and X-linked intellectual disability: four decades of discovery. *Am. J. Hum. Genet.*, **90**, 579–590.
10. Rogner, U.C., Heiss, N.S., Kioschis, P., Wiemann, S., Korn, B. and Poustka, A. (1996) Transcriptional analysis of the candidate region for incontinentia pigmenti (IP2) in Xq28. *Genome Res.*, **6**, 922–934.
11. Heiss, N.S. and Poustka, A. (1997) Genomic structure of a novel chloride channel gene, CLIC2, in Xq28. *Genomics*, **45**, 224–228.
12. Dulhunty, A.F., Pouliquin, P., Coggan, M., Gage, P.W. and Board, P.G. (2005) A recently identified member of the glutathione transferase structural family modifies cardiac RyR2 substate activity, coupled gating and activation by Ca2+ and ATP. *Biochem. J.*, **390**, 333–343.
13. Dulhunty, A.F., Hewawasam, R., Liu, D., Casarotto, M.G. and Board, P.G. (2011) Regulation of the cardiac muscle ryanodine receptor by glutathione transferases. *Drug Metab. Rev.*, **43**, 236–252.
14. Meng, X., Wang, G., Viero, C., Wang, Q., Mi, W., Su, X.D., Wagenknecht, T., Williams, A.J., Liu, Z. and Yin, C.C. (2009) CLIC2-RyR1 interaction and structural characterization by cryo-electron microscopy. *J. Mol. Biol.*, **387**, 320–334.
15. Goussakov, I., Miller, M.B. and Stutzmann, G.E. (2010) NMDA-mediated Ca(2+) influx drives aberrant ryanodine receptor activation in dendrites of young Alzheimer's disease mice. *J. Neurosci.*, **30**, 12128–12137.
16. Gant, J.C., Chen, K.C., Norris, C.M., Kadish, I., Thibault, O., Blalock, E.M., Porter, N.M. and Landfield, P.W. (2011) Disrupting function of FK506-binding protein 1b/12.6 induces the Ca^{2+}-dysregulation aging phenotype in hippocampal neurons. *J. Neurosci.*, **31**, 1693–1703.
17. Tarpey, P.S., Smith, R., Pleasance, E., Whibley, A., Edkins, S., Hardy, C., O'Meara, S., Latimer, C., Dicks, E., Menzies, A. *et al.* (2009) A systematic, large-scale resequencing screen of X-chromosome coding exons in mental retardation. *Nat. Genet.*, **41**, 535–543.
18. Liauw, J., Hoang, S., Choi, M., Eroglu, C., Sun, G.H., Percy, M., Wildman-Tobriner, B., Bliss, T., Guzman, R.G., Barres, B.A. *et al.* (2008) Thrombospondins 1 and 2 are necessary for synaptic plasticity and functional recovery after stroke. *J. Cereb. Blood Flow Metab.*, **28**, 1722–1732.
19. Christopherson, K.S., Ullian, E.M., Stokes, C.C., Mullowney, C.E., Hell, J.W., Agah, A., Lawler, J., Mosher, D.F., Bornstein, P. and Barres, B.A. (2005) Thrombospondins are astrocyte-secreted proteins that promote CNS synaptogenesis. *Cell*, **120**, 421–433.
20. Doornbos, M., Sikkema-Raddatz, B., Ruijvenkamp, C.A., Dijkhuizen, T., Bijlsma, E.K., Gijsbers, A.C., Hilhorst-Hofstee, Y., Hordijk, R., Verbruggen, K.T., Kerstjens-Frederikse, W.S. *et al.* (2009) Nine patients with a microdeletion 15q11.2 between breakpoints 1 and 2 of the Prader-Willi critical region, possibly associated with behavioural disturbances. *Eur. J. Med. Genet.*, **52**, 108–115.
21. von der Lippe, C., Rustad, C., Heimdal, K. and Rodningen, O.K. (2011) 15q11.2 microdeletion—seven new patients with delayed development and/or behavioural problems. *Eur. J. Med. Genet.*, **54**, 357–360.
22. Burnside, R.D., Pasion, R., Mikhail, F.M., Carroll, A.J., Robin, N.H., Youngs, E.L., Gadi, I.K., Keitges, E., Jaswaney, V.L., Papenhausen, P.R. *et al.* (2011) Microdeletion/microduplication of proximal 15q11.2 between BP1 and BP2: a susceptibility region for neurological dysfunction including developmental and language delay. *Hum. Genet.*, **130**, 517–528.
23. de Kovel, C.G., Trucks, H., Helbig, I., Mefford, H.C., Baker, C., Leu, C., Kluck, C., Muhle, H., von Spiczak, S., Ostertag, P. *et al.* (2010) Recurrent microdeletions at 15q11.2 and 16p13.11 predispose to idiopathic generalized epilepsies. *Brain*, **133**, 23–32.
24. Board, P.G., Coggan, M., Watson, S., Gage, P.W. and Dulhunty, A.F. (2004) CLIC-2 modulates cardiac ryanodine receptor Ca2+ release channels. *Int. J. Biochem. Cell Biol.*, **36**, 1599–1612.
25. Mi, W., Liang, Y.H., Li, L. and Su, X.D. (2008) The crystal structure of human chloride intracellular channel protein 2: a disulfide bond with functional implications. *Proteins*, **71**, 509–513.
26. Witham, S., Takano, K., Schwartz, C. and Alexov, E. (2011) A missense mutation in CLIC2 associated with intellectual disability is predicted by in silico modeling to affect protein stability and dynamics. *Proteins*, **79**, 2444–2454.
27. Jalilian, C., Gallant, E.M., Board, P.G. and Dulhunty, A.F. (2008) Redox potential and the response of cardiac ryanodine receptors to CLIC-2, a member of the glutathione S-transferase structural family. *Antioxid. Redox. Signal.*, **10**, 1675–1686.
28. Cromer, B.A., Gorman, M.A., Hansen, G., Adams, J.J., Coggan, M., Littler, D.R., Brown, L.J., Mazzanti, M., Breit, S.N., Curmi, P.M. *et al.* (2007) Structure of the Janus protein human CLIC2. *J. Mol. Biol.*, **374**, 719–731.
29. Chadwick, W., Brenneman, R., Martin, B. and Maudsley, S. (2010) Complex and multidimensional lipid raft alterations in a murine model of Alzheimer's disease. *Int. J. Alzheimers Dis.*, **2010**, 604792.
30. Everitt, A.B., Seymour, V.A., Curmi, J., Laver, D.R., Gage, P.W. and Tierney, M.L. (2009) Protein interactions involving the gamma2 large cytoplasmic loop of GABA(A) receptors modulate conductance. *FASEB J.*, **23**, 4361–4369.
31. Yin, C.C., Han, H., Wei, R. and Lai, F.A. (2005) Two-dimensional crystallization of the ryanodine receptor Ca2+ release channel on lipid membranes. *J. Struct. Biol.*, **149**, 219–224.
32. Kass, R.S. (2005) The channelopathies: novel insights into molecular and genetic mechanisms of human disease. *J. Clin. Invest.*, **115**, 1986–1989.
33. Catterall, W.A. (2011) Voltage-gated calcium channels. *Cold Spring Harb. Perspect. Biol.*, **3**, a003947.
34. George, C.H., Jundi, H., Thomas, N.L., Fry, D.L. and Lai, F.A. (2007) Ryanodine receptors and ventricular arrhythmias: emerging trends in mutations, mechanisms and therapies. *J. Mol. Cell Cardiol.*, **42**, 34–50.
35. Betzenhauser, M.J. and Marks, A.R. (2010) Ryanodine receptor channelopathies. *Pflugers Arch.*, **460**, 467–480.
36. Nagrani, T., Siyamwala, M., Vahid, G. and Bekheit, S. (2011) Ryanodine calcium channel: a novel channelopathy for seizures. *Neurologist*, **17**, 91–94.
37. Nakanishi, S., Kuwajima, G. and Mikoshiba, K. (1992) Immunohistochemical localization of ryanodine receptors in mouse central nervous system. *Neurosci. Res.*, **15**, 130–142.
38. Lai, F.A., Dent, M., Wickenden, C., Xu, L., Kumari, G., Misra, M., Lee, H.B., Sar, M. and Meissner, G. (1992) Expression of a cardiac

Ca(2+)-release channel isoform in mammalian brain. *Biochem. J.*, **288** (Pt 2), 553–564.
39. Furuichi, T., Furutama, D., Hakamata, Y., Nakai, J., Takeshima, H. and Mikoshiba, K. (1994) Multiple types of ryanodine receptor/Ca2+ release channels are differentially expressed in rabbit brain. *J. Neurosci.*, **14**, 4794–4805.
40. Hakamata, Y., Nakai, J., Takeshima, H. and Imoto, K. (1992) Primary structure and distribution of a novel ryanodine receptor/calcium release channel from rabbit brain. *FEBS Lett.*, **312**, 229–235.
41. Futatsugi, A., Kato, K., Ogura, H., Li, S.T., Nagata, E., Kuwajima, G., Tanaka, K., Itohara, S. and Mikoshiba, K. (1999) Facilitation of NMDAR-independent LTP and spatial learning in mutant mice lacking ryanodine receptor type 3. *Neuron*, **24**, 701–713.
42. Balschun, D., Wolfer, D.P., Bertocchini, F., Barone, V., Conti, A., Zuschratter, W., Missiaen, L., Lipp, H.P., Frey, J.U. and Sorrentino, V. (1999) Deletion of the ryanodine receptor type 3 (RyR3) impairs forms of synaptic plasticity and spatial learning. *EMBO J.*, **18**, 5264–5273.
43. Mamanova, L., Coffey, A.J., Scott, C.E., Kozarewa, I., Turner, E.H., Kumar, A., Howard, E., Shendure, J. and Turner, D.J. (2010) Target-enrichment strategies for next-generation sequencing. *Nat. Methods*, **7**, 111–118.
44. Baker, R.T., Catanzariti, A.M., Karunasekara, Y., Soboleva, T.A., Sharwood, R., Whitney, S. and Board, P.G. (2005) Using deubiquitylating enzymes as research tools. *Methods Enzymol.*, **398**, 540–554.
45. Niesen, F.H., Berglund, H. and Vedadi, M. (2007) The use of differential scanning fluorimetry to detect ligand interactions that promote protein stability. *Nat. Protoc.*, **2**, 2212–2221.
46. Laver, D.R., Roden, L.D., Ahern, G.P., Eager, K.R., Junankar, P.R. and Dulhunty, A.F. (1995) Cytoplasmic Ca2+ inhibits the ryanodine receptor from cardiac muscle. *J. Membr. Biol.*, **147**, 7–22.
47. Ahern, G.P., Junankar, P.R. and Dulhunty, A.F. (1994) Single channel activity of the ryanodine receptor calcium release channel is modulated by FK-506. *FEBS Lett.*, **352**, 369–374.
48. Dulhunty, A., Gage, P., Curtis, S., Chelvanayagam, G. and Board, P. (2001) The glutathione transferase structural family includes a nuclear chloride channel and a ryanodine receptor calcium release channel modulator. *J. Biol. Chem.*, **276**, 3319–3323.
49. Abdellatif, Y., Liu, D., Gallant, E.M., Gage, P.W., Board, P.G. and Dulhunty, A.F. (2007) The Mu class glutathione transferase is abundant in striated muscle and is an isoform-specific regulator of ryanodine receptor calcium channels. *Cell Calcium*, **41**, 429–440.
50. Wei, L., Abdellatif, Y.A., Liu, D., Kimura, T., Coggan, M., Gallant, E.M., Beard, N.A., Board, P.G. and Dulhunty, A.F. (2008) Muscle-specific GSTM2–2 on the luminal side of the sarcoplasmic reticulum modifies RyR ion channel activity. *Int. J. Biochem. Cell Biol.*, **40**, 1616–1628.
51. Hewawasam, R., Liu, D., Casarotto, M.G., Dulhunty, A.F. and Board, P.G. (2011) The structure of the C-terminal helical bundle in glutathione transferase M2–2 determines its ability to inhibit the cardiac ryanodine receptor. *Biochem. Pharmacol.*, **80**, 381–388.
52. Serysheva, I.I., Ludtke, S.J., Baker, M.L., Cong, Y., Topf, M., Eramian, D., Sali, A., Hamilton, S.L. and Chiu, W. (2008) Subnanometer-resolution electron cryomicroscopy-based domain models for the cytoplasmic region of skeletal muscle RyR channel. *Proc. Natl. Acad. Sci. USA*, 105, 9610–9615.
53. Mintseris, J., Pierce, B., Wiehe, K., Anderson, R., Chen, R. and Weng, Z. (2007) Integrating statistical pair potentials into protein complex prediction. *Proteins*, **69**, 511–520.
54. Pierce, B.G., Hourai, Y. and Weng, Z. (2011) Accelerating protein docking in ZDOCK using an advanced 3D convolution library. *PLoS One*, **6**, e24657.
55. Zhang, Z., Teng, S., Wang, L., Schwartz, C.E. and Alexov, E. (2010) Computational analysis of missense mutations causing Snyder-Robinson syndrome. *Hum. Mutat.*, **31**, 1043–1049.
56. Teng, S., Madej, T., Panchenko, A. and Alexov, E. (2009) Modeling effects of human single nucleotide polymorphisms on protein-protein interactions. *Biophys. J.*, **96**, 2178–2188.
57. Zhang, Z., Norris, J., Schwartz, C. and Alexov, E. (2011) In silico and in vitro investigations of the mutability of disease-causing missense mutation sites in spermine synthase. *PLoS One*, 6, e20373.
58. Tae, H.S., Cui, Y., Karunasekara, Y., Board, P.G., Dulhunty, A.F. and Casarotto, M.G. (2011) Cyclization of the intrinsically disordered alpha1S dihydropyridine receptor II-III loop enhances secondary structure and in vitro function. *J. Biol. Chem.*, **286**, 22589–22599.